SVIP Is a Novel VCP/p97-interacting Protein Whose Expression Causes Cell Vacuolation

Masami Nagahama,*† Mie Suzuki,*† Yuko Hamada,* Kiyotaka Hatsuzawa,* Katsuko Tani,* Akitsugu Yamamoto,‡ and Mitsuo Tagaya*§

*School of Life Science, Tokyo University of Pharmacy and Life Science, Hachioji, Tokyo 192-0392, Japan; and ‡Department of Physiology, Kansai Medical University, Moriguchi, Osaka 570-8506, Japan

VCP/p97 is involved in a variety of cellular processes, including membrane fusion and ubiquitin-dependent protein degradation. It has been suggested that adaptor proteins such as p47 and Ufd1p confer functional versatility to VCP/p97. To identify novel adaptors, we searched for proteins that interact specifically with VCP/p97 by using the yeast two-hybrid system, and discovered a novel VCP/p97-interacting protein named *s*mall *VCP/p97-i*nteracting *p*rotein (SVIP). Rat SVIP is a 76-amino acid protein that contains two putative coiled-coil regions, and potential myristoylation and palmitoylation sites at the N terminus. Binding experiments revealed that the N-terminal coiled-coil region of SVIP, and the N-terminal and subsequent ATP-binding regions (ND1 domain) of VCP/p97, interact with each other. SVIP and previously identified adaptors p47 and ufd1p interact with VCP/p97 in a mutually exclusive manner. Overexpression of full-length SVIP or a truncated mutant did not markedly affect the structure of the Golgi apparatus, but caused extensive cell vacuolation reminiscent of that seen upon the expression of VCP/p97 mutants or polyglutamine proteins in neuronal cells. The vacuoles seemed to be derived from endoplasmic reticulum membranes. These results together suggest that SVIP is a novelVCP/p97 adaptor whose function is related to the integrity of the endoplasmic reticulum.

INTRODUCTION

VCP/p97 is involved in remarkably diverse processes in cells. Mammalian VCP/p97 and its yeast counterpart Cdc48p participate in the formation of organelles, including the endoplasmic reticulum (ER), Golgi apparatus, and nuclear envelope (Zhang et al., 1994; Acharya et al., 1995; Latterich et al., 1995; Rabouille et al., 1995; Lavoie et al., 2000; Roy et al., 2000; Hetzer et al., 2001), in ubiquitin-dependent proteolysis (Ghislain et al., 1996; Dai et al., 1998; Yen et al., 2000; Dai and Li, 2001; Rape et al., 2001; Braun et al., 2002; Rabinovich et al., 2002), and in retrograde transport from the ER to the cytosol (Ye et al., 2001; Jarosch et al., 2002). Mammalian VCP/p97 is also involved in STAT3-mediated cell cycle progression (Shirogane et al., 1999) and in lymphocyte stimulation (Egerton et al., 1992; Schulte et al., 1994). In addition, it interacts with functionally unrelated proteins such as clathrin (Pleasure et al., 1993), testis brain RNA-binding protein (Wu et al., 1999), a breast/ovarian cancer susceptibility gene product, BRCA1 (Zhang et al., 2000b), glucosamine-6-phosphate acetyltransferase EMeg32 (Boehmelt et al., 2000), and synaptotagmin (Sugita and Südhof, 2000), although the physiological significance of these interactions is obscure at present. A *Drosophila* VCP/p97 ortholog is required for the formation of the fusome, a germ cell line-specific organelle (Leon and McKearin, 1999), and *oskar* mRNA localization in the egg chamber (Ruden et al., 2000). *Xenopus* VCP/p97 may function in DNA replication through interaction with a DNA unwinding factor (Yamada et al., 2000).

The functional versatility of VCP/p97 can be at least partly explained by its chaperone-like activity. VCP/p97 is a member of the AAA (ATPases associated with diverse cellular activities) family, which is characterized by the presence of one or two conserved ATP-binding domains consisting of ~200 amino acid residues (Confalonieri and Duguet, 1995; Patel and Latterich, 1998; Ogura and Wilkinson, 2001). Many AAA family proteins are hexameric (Vale, 2000; Ogura and Wilkinson, 2001) and undergo conformational changes upon the binding and/or hydrolysis of ATP (Hanson et al., 1997; Rouiller et al., 2000). It has been proposed that

AAA family proteins coupled with the binding and/or hydrolysis of ATP participate in the assembly, disassembly, and operation of protein complexes (Confalonieri and Duguet, 1995; Morgan and Burgoyne, 1995; Neuwald *et al.*, 1999; Rouiller *et al.*, 2000). Indeed, several AAA family proteins, including VAT, the archaeal ortholog of VCP/p97, exhibit such activity (Cruciat *et al.*, 1999; Golbik *et al.*, 1999; Leonhard *et al.*, 1999).

The presence of multiple adaptors for VCP/p97 may also contribute to the functional versatility of VCP/p97. p47 binds to VCP/p97 (Kondo *et al.*, 1997), and the VCP/p97-p47 complex associates with Golgi membranes via syntaxin 5 and mediates Golgi assembly during mitosis (Rabouille *et al.*, 1998). In the ubiquitin-dependent pathway, Cdc48p functions with Ufd2p (Koegl *et al.*, 1999) and Ufd3p (Ghislain *et al.*, 1996), both of which are involved in the UFD pathway (Johnson *et al.*, 1995). Ufd1p, another protein involved in the UFD pathway, together with Npl4p, a protein required for nuclear envelope integrity (DeHoratius and Silver, 1996), also forms a complex with VCP/p97 (Meyer *et al.*, 2000), and the complex participates in ubiquitin-dependent protein processing or degradation of ER proteins (Bays *et al.*, 2001; Hitchcock *et al.*, 2001; Rape *et al.*, 2001; Ye *et al.*, 2001; Braun *et al.*, 2002; Jarosch *et al.*, 2002). The fact that the binding of p47 and Ufd1p to VCP/p97 is mutually exclusive suggests that the adaptor proteins direct VCP/p97 basic activity in different cellular pathways (Meyer *et al.*, 2000).

With the hope of finding new adaptors for VCP/p97, we performed yeast two-hybrid screening by using the full-length VCP/p97 as bait. We found a protein named *s*mall *VCP/p97-i*nteracting *p*rotein (SVIP) consisting of 76 amino acids with two putative coiled-coil regions. Overexpression of SVIP caused the formation of large vacuoles that seemed to be derived from the ER.

MATERIALS AND METHODS

Materials

Glutathione-Sepharose 4B, cyanogen bromide-activated Sepharose 4B, and benzamidine-Sepharose 6B were obtained from Amersham Biosciences (Piscataway, NJ). Ni^{2+}-nitrilotriacetic acid-agarose was obtained from QIAGEN (Valencia, CA). LipofectAMINE PLUS reagent was obtained from Invitrogen (Carlsbad, CA). Digitonin was purchased from Merck (Darmstadt, Germany). Transferrin and medium for cell culture were obtained from Sigma-Aldrich (St. Louis, MO). LysoTracker and lucifer yellow were purchased from Molecular Probes (Eugene, OR).

Antibodies

Polyclonal antiserum against SVIP was raised against the full-length SVIP fused to the C terminus of glutathione *S*-transferase (GST). An antibody against GST-SVIP was purified by affinity chromatography on antigen-coupled beads. Components reactive to GST in the purified anti-GST-SVIP antibodies were removed by passage through a column of GST-coupled beads. The polyclonal anti-p47 antibody was a generous gift from Dr. G. Warren (Yale University, New Haven, CT). Polyclonal anti-mannosidase II and anti-β-COP antibodies were raised in this laboratory. A polyclonal antibody against NADPH-cytochrome P450 reductase (FP2) was prepared as described previously (Masaki *et al.*, 1987). Monoclonal anti-calnexin, anti-γ-adaptin, and anti-Ufd1p antibodies were obtained from Transduction Laboratories (Lexington, KY). Monoclonal antibodies against GST and BiP (anti-KDEL) were obtained from Amersham

Biosciences and StressGen (Victoria, British Columbia, Canada), respectively. Polyclonal and monoclonal anti-FLAG antibodies were purchased from Zymed Laboratories (South San Francisco, CA) and Sigma-Aldrich, respectively. Polyclonal antibodies against transferrin and lucifer yellow were purchased from DAKO Japan (Kyoto, Japan) and Molecular Probes, respectively.

Two-Hybrid Screening and Sequencing

The full-length cDNA of rat VCP/p97 was cloned into the *Sma*I/*Sal*I sites of pGBT9, and the resultant plasmid (pGBT-VCP/p97) was transformed into yeast strain HF7c. Yeast two-hybrid screening was carried out essentially according to the manufacturer's protocol by using a GAL4 DNA activation domain fusion library in pGAD10 (MATCHMAKER rat brain cDNA library; BD Biosciences Clontech, Palo Alto, CA). Positive clones were isolated by growth selection on plates lacking Trp, Leu, and His, followed by β-galactosidase filter assays. The isolated clones were sequenced with an automated DNA sequencer (ABI PRISMTM377; Applied Biosystems, Union City, CA).

Subcellular Fractionation

Subcellular fractionation was conducted essentially as described previously (Hatsuzawa *et al.*, 2000).

Expression and Purification of Proteins

A bacterial expression plasmid for N-terminally hexahistidine-tagged VCP/p97 (His-VCP/p97) was constructed by subcloning the full-length cDNA of rat VCP/p97 into pQE30 (QIAGEN). The bacterial expression plasmid for N-terminally hexahistidine-tagged Ufd1p (His-Ufd1p) was kindly donated by Dr. G. Warren. Recombinant His-tagged proteins were expressed in *Escherichia coli* after induction with isopropyl-1-thio-β-ᴅ-galactoside and purified by Ni^{2+}-nitrilotriacetic acid-agarose chromatography.

Expression plasmids for SVIP and p47 fused to the N-terminal GST were constructed by subcloning their cDNAs into the bacterial expression pGEX vector (Amersham Biosciences). Recombinant GST-fusion proteins were expressed in *E. coli* and purified by glutathione-Sepharose 4B chromatography. Untagged p47 was prepared by cleavage of GST-p47 with thrombin and purified by passage through glutathione-Sepharose 4B and benzamidine-Sepharose columns.

Binding Assays

The mammalian expression plasmids pEBG (Tanaka *et al.*, 1995) and pFLAG-CMV-2 (Sigma-Aldrich) were used to express proteins (SVIP, VCP/p97, p47, and Ufd1p) fused to the N-terminal GST and FLAG, respectively. To perform in vivo binding assays, 293Tcells grown in DMEM supplemented with 10% fetal bovine serum were transfected with expression plasmids by using LipofectAMINE PLUS reagent. At 40 h after transfection, the cells were harvested and lysed in lysis buffer (0.3 ml/35-mm dish) consisting of 20 mM HEPES-KOH (pH 7.4), 100 mM KCl, 2 mM EDTA, 1 mM phenylmethylsulfonyl fluoride, 1 mM dithiothreitol, 10 μg/ml leupeptin, 1 μg/ml pepstatin A, 1% Trasylol (aprotinin solution; Bayer AG, Wuppertal, Germany), and 1% Triton X-100. The lysates were centrifuged in a microfuge for 20 min at 14,000 rpm to remove insoluble materials. To each supernatant (270 μl) was added 230 μl of lysis buffer, and the mixture was incubated with glutathione-Sepharose 4B beads for 2 h with gentle rotating. The beads were sedimented in a microfuge and then washed four times with lysis buffer. The materials pulled down with the beads were dissociated from the beads by boiling in SDS-PAGE sample buffer. An equal volume of 2× SDS-PAGE sample buffer was mixed with 4.4% (12 μl) of the total lysate, followed by heating at 95°C for 5 min. Samples were resolved by SDS-PAGE on 12.5% gels, blotted and then immunostained with appropriate antibodies by using an enhanced chemiluminescence reagent (Pierce Chemical, Rockford, IL).
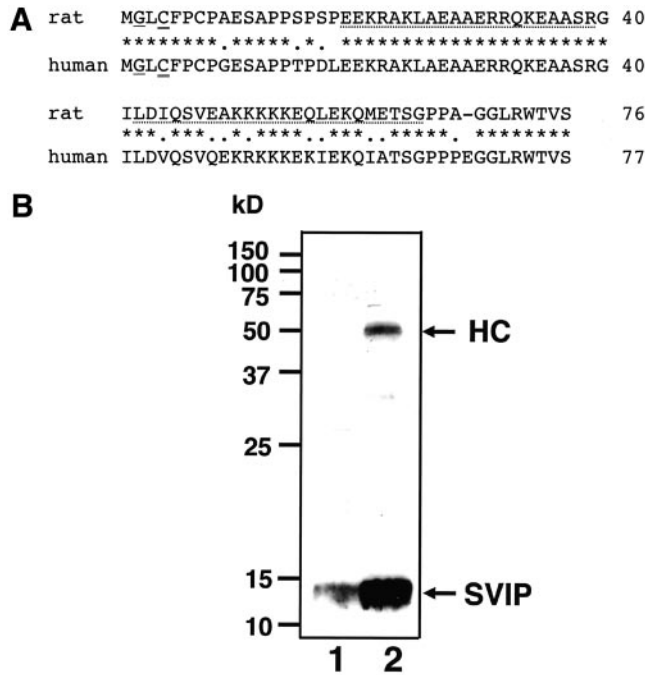
A

```
rat     MGLCFPCPAESAPPSPSPEEKRAKLAEAAERRQKEAASRG 40
        *******.*****.*. ********************
human   MGLCFPCPGESAPPTPDLEEKRAKLAEAAERRQKEAASRG 40

rat     ILDIQSVEAKKKKKEQLEKQMETSGPPA-GGLRWTVS     76
        ***.***..*.****..***..*****. *******
human   ILDVQSVQEKRKKKEKIEKQIATSGPPPEGGLRWTVS     77
```

B

Figure 1. Structure and expression of SVIP. (A) Amino acid sequence of rat SVIP is compared with that of human SVIP. A putative myristoylation site (Gly-2) and a palmitoylation site (Cys-4) are underlined and double underlined, respectively. Stars and dots represent identical and similar amino acid residues, respectively. Putative coiled-coil sequences are dot underlined. (B) Expression of SVIP in 293T cells. A 293T cell lysate (~50 μg of protein) was analyzed by immunoblotting with the anti-SVIP antibody (lane 1). Alternatively, a 293T cell lysate (~1 mg of protein) was subjected to immunoprecipitation with the anti-SVIP antibody, and the precipitated proteins were detected by immunoblotting with the same antibody (lane 2). HC, heavy chain of immunoglobulin. The molecular size markers are indicated on the left.

Binding experiments with purified proteins were carried out essentially as described previously (Meyer *et al.*, 2000). Two micrograms of GST-SVIP was incubated with 4 μg of His-VCP/p97 in the presence of a 0, 1, 5, or 25 M excess of p47 or His-Ufd1p and then pulled down with glutathione-Sepharose 4B. The precipitated materials were separated by SDS-PAGE and detected by Coomassie Blue R-250 staining.

Immunofluorescence

Immunofluorescence microscopy was performed as described previously (Tagaya *et al.*, 1996). HeLa cells were transfected with the plasmid for the full-length or mutant SVIP fused to the C-terminal FLAG, or p47 or Ufd1p fused to the N-terminal FLAG. After 24 h, the cells were immediately fixed or treated as described in the legends to the figures and then processed for immunofluorescence analysis.

Electron Microscopy

HeLa cells cultured on plastic coverslips were fixed in 2.5% glutaraldehyde in 0.1 M sodium phosphate buffer (pH 7.4) for 2 h and then processed as described previously (Yamaguchi *et al.*, 1997). For immunoelectron microscopy, the preembedding silver or gold enhancement immunogold method described by Nakamura *et al.*
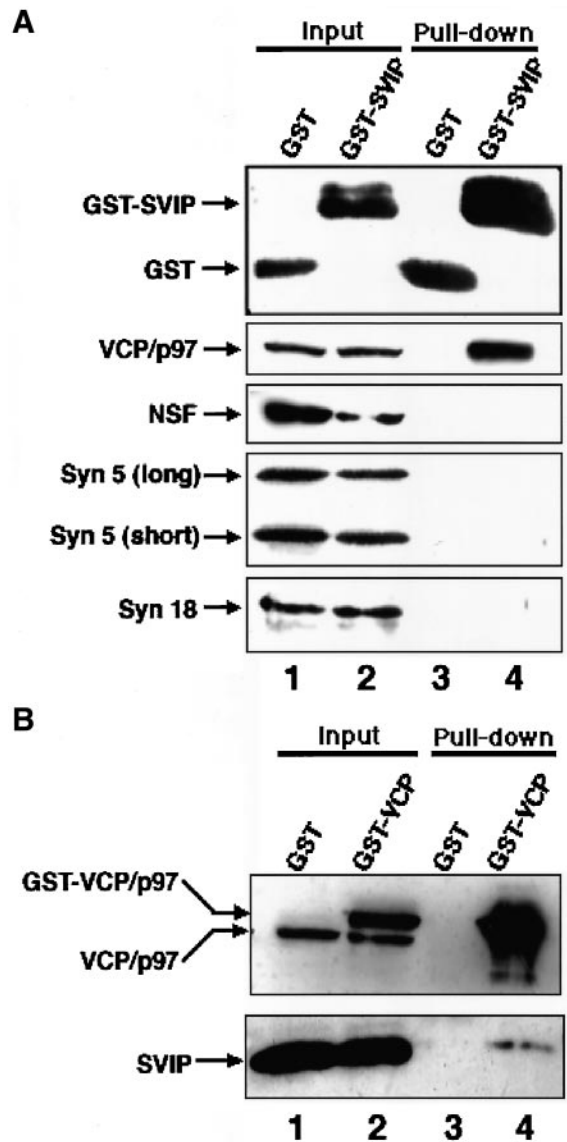
A

B

Figure 2. Binding between VCP/p97 and SVIP. (A) GST or GST-SVIP was expressed in 293T cells and then the cells were lysed. After centrifugation, GST (lane 1) or GST-SVIP (lane 2) in the supernatant was pulled down with glutathione beads. The proteins coprecipitated with GST (lane 3) or GST-SVIP (lane 4) were detected by immunoblotting with antibodies against proteins as indicated on the left. The amount of each protein in 4.4% of the supernatant is shown (input). (B) Expressed GST (lane 1) or GST-VCP/p97 (lane 2) was pulled down with glutathione beads, and the proteins coprecipitated with GST (lane 3) and GST-VCP/p97 (lane 4) were detected by immunoblotting with antibodies against VCP/p97 and SVIP. The amounts of GST-VCP/p97, endogenous VCP/p97, and endogenous SVIP in 4.4% of the supernatant used are shown (input).

(2000) was used. For the detection of FP2, cells were fixed in 4% paraformaldehyde in 0.1 M sodium phosphate buffer (pH 7.4) for 2 h. The cells were frozen in 14% glycerol and 35% sucrose in liquid nitrogen and then thawed. They were incubated with the anti-NADPH-cytochrome P450 reductase polyclonal antibodies and then
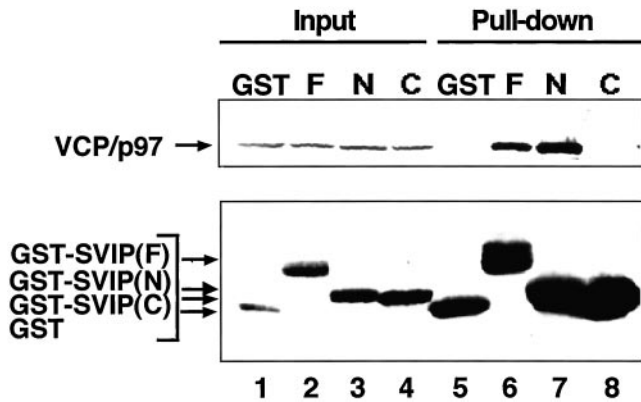
Figure 3. The N-terminal region of SVIP interacts with VCP/p97. GST (GST), or the full-length (F), residues 1–39 (N), or residues 40–76 (C) of SVIP fused to GST were expressed in 293T cells. Supernatants of cell lysates were prepared, and the GST proteins were pulled down with glutathione beads. The precipitated proteins were detected by immunoblotting with antibodies against GST and VCP/p97 (pull-down; lanes 5–8). The amounts of endogenous VCP/p97 and GST-SVIP fusion proteins in 4.4% of the supernatant used are shown (input; lanes 1–4).

with colloidal gold (1.4-nm-diameter)–conjugated secondary antibodies. The gold labeling was intensified using a silver enhancement kit (HQ silver; Nanoprobes, Yaphank, NY). For the detection of BiP, fixed cells were permeabilized with 0.25% saponin for 30 min, and reacted with the anti-BiP monoclonal antibodies and then with colloidal gold (1.4-nm-diamater)–conjugated secondary antibodies. The gold labeling was intensified using a gold enhancement kit (Nanoprobes).

RESULTS

Identification of SVIP

To identify novel adaptors for VCP/p97, we screened a rat brain cDNA library by using the full-length VCP/p97 cDNA as bait in the yeast two-hybrid system. Two types of transformants that grew in His-medium and exhibited β-galactosidase activity were obtained. One clone encoded p47, which is known to bind VCP/p97 (Kondo *et al.*, 1997). The other encoded a novel protein with two putative coiled-coil regions. We named this protein SVIP. Because none of the obtained cDNA clones seemed to contain the entire coding region of SVIP, we searched the extended sequence tag (EST) database and found many human EST clones. Some of them (GenBank accession numbers BI464525, BI667146, BI765368, BF031998, BG501588, and BG706666) seemed to encode full-length SVIP because a putative termination codon is present 5′ upstream of the coding sequence of each clone. A human genome database search revealed that the gene of SVIP is located on chromosome 11 and that the termination codon 5′ upstream of the coding sequence is present in the genome sequence as observed in the EST sequences. These findings suggest that the longest 5′ cDNA clone obtained in the two-hybrid screening encodes rat SVIP starting from Glu-10. Northern blot analysis with a probe specific for SVIP showed that it is expressed ubiquitously
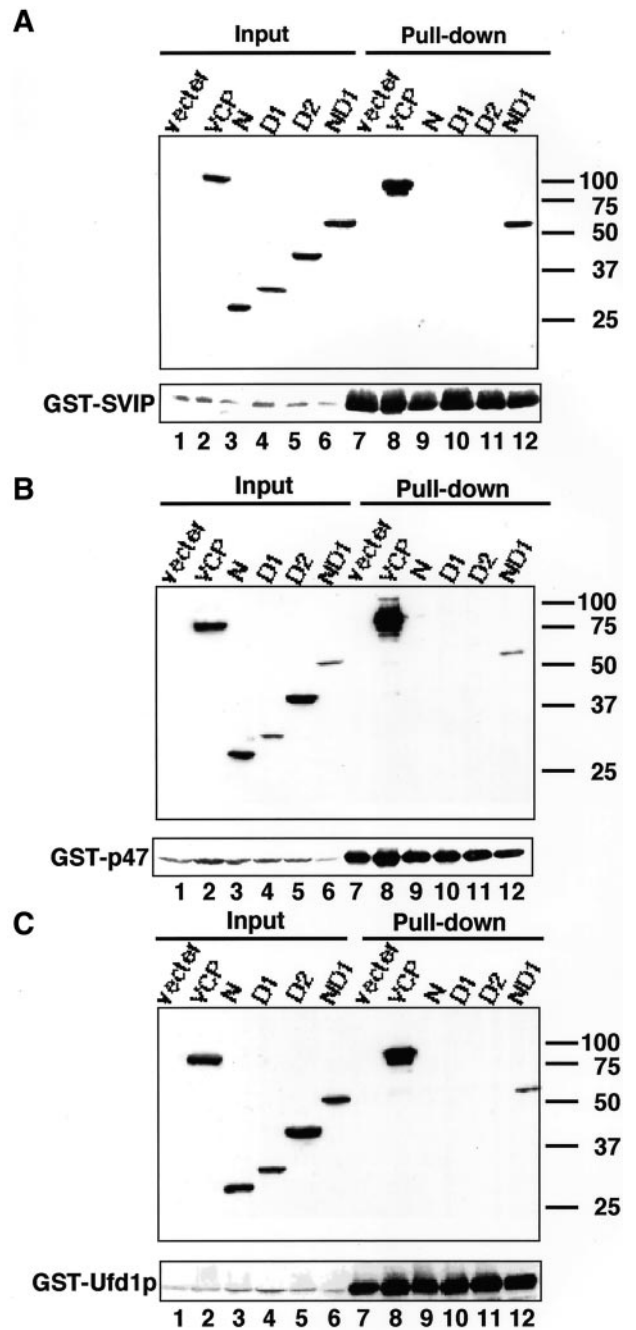

Figure 4. The N-terminal and subsequent ATP-binding regions of VCP/p97 participate in the interaction with adaptor proteins. VCP/p97, or the N-terminal domain (residues 1–202), D1 domain (residues 203–450), D2 domain (residues 451–807), or ND1 domain (residues 1–450) of VCP/p97 was expressed as a FLAG-tagged protein in 293T cells. As a control, cells were transfected with the vector used for the expression of VCP/p97 constructs (vector). Simultaneously, GST-SVIP (A), GST-p47 (B), or GST-Ufd1p (C) was expressed. Supernatants of cell lysates were prepared, and the GST proteins were pulled down with glutathione beads. The precipitated proteins were detected by immunoblotting with antibodies against GST and FLAG (pull-down; lanes 7–12). The amounts of FLAG and GST constructs in 4.4% of the supernatant used are shown (input; lanes 1–6).
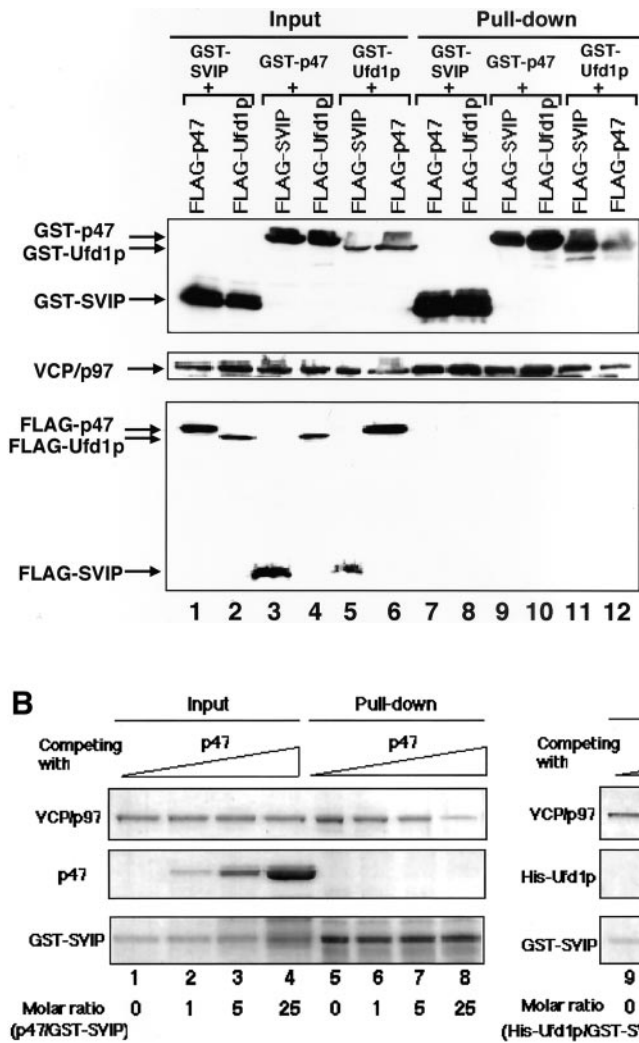
Figure 5. SVIP, p47, and Ufd1p interact with VCP/p97 in a mutually exclusive manner. (A) Pull-down experiments. GST-SVIP was coexpressed with FLAG-tagged p47 or FLAG-tagged Ufd1p in 293T cells. Supernatants of cell lysates were prepared, and the GST-SVIP was pulled down with glutathione beads. The precipitated endogenous VCP/p97, GST-SVIP, FLAG-p47, and FLAG-Ufd1p were detected by immunoblotting (lanes 7 and 8). The amounts of endogenous VCP/p97 and expressed proteins in 4.4% of the supernatant used are shown (lanes 1 and 2). Alternatively, GST-p47 was coexpressed with FLAG-SVIP or FLAG-Ufd1p (lanes 3, 4, 9, and 10), or GST-Ufd1p was coexpressed with FLAG-SVIP or FLAG-p47 (lanes 5, 6, 11, and 12), and then pull-down experiments were performed. (B) Competition experiments. GST-SVIP was incubated with His-VCP/p97 in the absence or presence of increasing amounts of p47 or His-Ufd1p (molar excess: 0, 1, 5 and 25 times), as indicated. GST-SVIP was pulled down with glutathione beads, and the precipitated proteins were detected by SDS-PAGE followed by Coomassie Brilliant Blue staining (pull-down). The amounts of added proteins in 10% of the reaction mixtures are shown (input).

(our unpublished data). Human and rat SVIPs consist of 77 and 76 amino acid residues, respectively, and exhibit 82% sequence identity (Figure 1A). SVIP exhibits no significant sequence homology with other proteins or motifs except for the presence of a putative myristoylation site (Gly-2) and a palmitoylation site (Cys-4) in the N-terminal region. Sequence analysis with COILS, a Lupas algorithm (Lupas *et al.*, 1991)-based program supplied on the EMBnet, with a 21-residue window predicted the presence of two coiled-coil regions (residues 19–39 and 42–65).

To confirm the existence of SVIP in mammalian cells, we raised a polyclonal antibody against bacterially expressed SVIP and carried out immunoblotting and immunoprecipitation of 293Tcell extracts. As shown in Figure 1B, a 13-kDa protein was specifically recognized and immunoprecipitated by the anti-SVIP antibody. The detected protein had a larger molecular size than that calculated from the predicted amino acid sequence (8.4 kDa for human SVIP). This discrepancy can be partly explained, as expected from its primary structure, by lipid modification of SVIP.

Interaction between VCP/p97 and SVIP

Because SVIP is a small protein consisting of two putative coiled-coil regions, it may interact nonspecifically with VCP/p97. To exclude this possibility, we examined the interaction of SVIP with another AAA protein, *N*-ethylmaleimide sensitive factor (NSF), and coiled-coil proteins syntaxin 5 and syntaxin 18 by using a yeast two-hybrid assay. The results showed that SVIP interacts with VCP/p97, but not with NSF, syntaxin 5, or syntaxin 18 (our unpublished data).

We next examined whether SVIP interacts with VCP/p97 in mammalian cells. For this purpose, GST-SVIP was expressed in 293T cells, and cell lysates were prepared and incubated with glutathione beads. The precipitated proteins were analyzed by immunoblotting. As shown in Figure 2A, endogenous VCP/p97 was pulled down with GST-SVIP (lane 4), whereas no precipitation of VCP/p97 was observed for GST (lane 3). Consistent with the results of the yeast two-hybrid analysis, NSF, syntaxin 5, and orsyntaxin 18 was
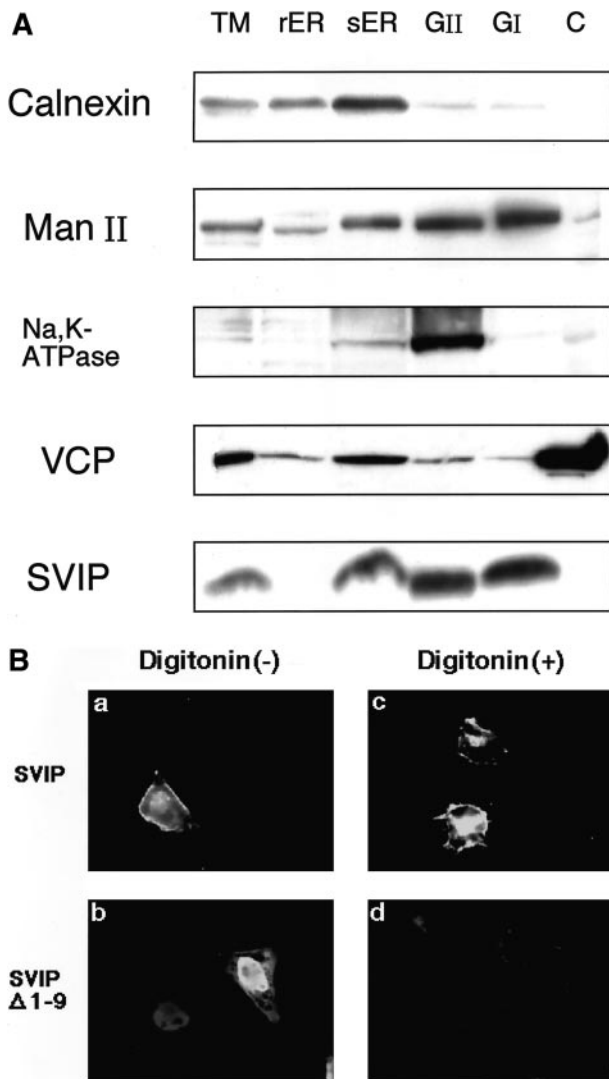
Figure 6. SVIP is associated with various membranes. (A) Rat liver extracts were separated by stepwise centrifugation. The total membrane fraction (TM), rough ER (rER), smooth ER (sER), GII, GI, and cytosol (C) were analyzed by immunoblotting with antibodies against calnexin (ER marker), mannosidase II (Man II, Golgi marker), Na$^+$,K$^+$-ATPase (plasma membrane marker), VCP/p97, and SVIP. (B) Full-length SVIP or SVIPΔ1–9 was expressed as a C-terminally FLAG-tagged protein in HeLa cells. The cells were permeabilized with digitonin as described previously (Tagaya et al., 1996) and then subjected to immunofluorescence analysis. Cells expressing the full-length SVIP were treated without digitonin (a) or with digitonin (c), and cells expressing the mutant SVIP were treated without digitonin (b) or with digitonin (d).

not coprecipitated with GST-SVIP. When the reverse experiment was conducted (Figure 2B), endogenous SVIP was pulled down with GST-VCP/p97 (lane 4), but not with GST (lane 3). These results suggest that SVIP interacts specifically with VCP/p97.

Regions Involved in Interaction between SVIP and VCP/p97

We next determined which region of SVIP is responsible for the interaction with VCP/p97. Because SVIP contains two putative coiled-coil regions, the N-terminal 39-amino acid residues including the first coiled-coil region and the C-terminal 37-amino acid residues including the second coiled-coil region were expressed as GST fusion proteins, and then pull-down experiments were performed. As shown in Figure 3, endogenous VCP/p97 was pulled down with the N-terminal construct (lane 7), but not with the C-terminal one (lane 8).

VCP/p97 comprises two AAA domains (D1 and D2) with an N-terminal domain (Koller and Brownstein, 1987; Zhang et al., 2000a). To define the binding site for SVIP on VCP/p97, the N-terminal domain (residues 1–202), D1 domain (residues 203–450), D2 domain (residues 451–807), or ND1 domain (residues 1–450) was expressed as a FLAG-tagged protein and SVIP was expressed as a GST fusion protein, and then pull-down assays were carried out. As shown in Figure 4A, SVIP was pulled down with the ND1 domain (lane 12), but not with the N-terminal domain (lane 9), D1 domain (lane 10), or D2 domain (lane 11).

SVIP Forms a Distinct Complex with VCP/p97 without p47 or Ufd1p

Previous studies showed that p47 and Ufd1p/Npl4p bind to VCP/p97 (Kondo et al., 1997; Meyer et al., 2000). Pull-down experiments similar to those performed for SVIP revealed that p47 and Ufd1p also bind to the ND1 domain of VCP/p97 (Figure 4, B and C). The fact that SVIP, p47, and Ufd1p occupy the same site on VCP/p97 raises the possibility that each adaptor protein forms a distinct complex with VCP/p97. To explore this possibility, GST-SVIP was coexpressed with FLAG-p47 or FLAG-Ufd1p and then pulled down with glutathione beads, and the precipitated materials were analyzed by immunoblotting. As shown in Figure 5A, neither-FLAG-p47 (lane 7) nor FLAG-Ufd1p (lane 8) was coprecipitated with GST-SVIP, although endogenous VCP/p97 was coprecipitated, suggesting that the VCP/p97-SVIP complex does not contain p47 or Ufd1p. Similar analyses demonstrated the absence of SVIP in the VCP/p97-p47 complex (Figure 5A, lane 9) or the VCP/p97-Ufd1p complex (Figure 5A, lane 11), and confirmed the previous finding that the binding of p47 and Ufd1p to VCP/p97 is mutually exclusive (Figure 5A, lanes 10 and 12) (Meyer et al., 2000).

To confirm that the binding of SVIP, p47, and Ufd1p to VCP/p97 is mutually exclusive, binding experiments with purified recombinant proteins were performed. GST-SVIP was incubated with His-VCP/p97 in the presence of increasing amounts of p47 and then pulled down with glutathione beads, and the coprecipitated His-VCP/p97 was analyzed. As shown in Figure 5B, the binding of His-VCP/p97 to GST-SVIP decreased in a dose-dependent manner with the addition of p47. Similarly, the binding of His-VCP/p97 to GST-SVIP was inhibited by the addition of His-Ufd1p. These results clearly demonstrated that VCP/p97 interacts with SVIP, p47, and Ufd1p in a mutually exclusive manner, and forms distinct complexes with these adaptor proteins both in vivo and in vitro.
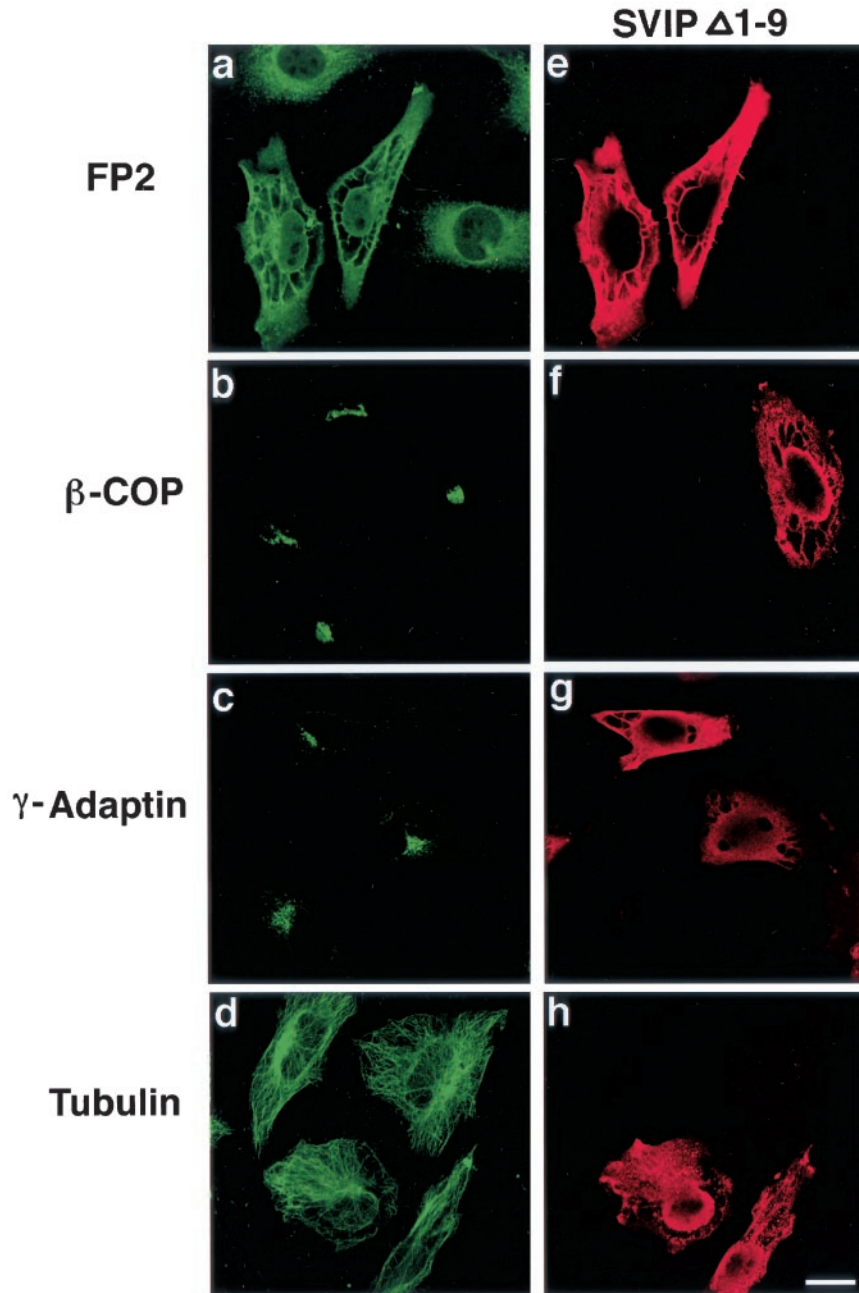
SVIP Δ1-9

Figure 7. Overexpression of SVIP causes the formation of vacuoles. HeLa cells were transfected with the plasmid for C-terminally FLAG-tagged SVIPΔ1-9. At 24 h after transfection, the cells were double immunostained with antibodies against an ER protein, FP2 (a), β-COP (b), γ-adaptin (c), or tubulin (d), and FLAG (e, f, g, and h).

Localization of SVIP

We next investigated the localization of SVIP. Rat liver membranes were fractionated by sucrose stepwise gradient centrifugation, and each fraction was analyzed by immunoblotting with antibodies against SVIP and organelle marker proteins. As shown in Figure 6A, SVIP was observed in the smooth ER and Golgi/plasma membrane fractions, but not in the cytosol. The protease sensitivity of SVIP suggests that it is peripherally associated with membranes (our unpublished data).

SVIP does not contain transmembrane regions, but possesses potential myristoylation and palmitoylation sites in the N-terminal region. To determine whether the membrane anchorage of SVIP is mediated by its N-terminal region, full-length SVIP or a mutant lacking the N-terminal nine residues (SVIPΔ1-9) was expressed as a C-terminally FLAG-tagged protein, and then the cells were treated with a low concentration of digitonin. Such treatment of cells allows cytosolic proteins, but not membrane proteins, to leak from the cells. As shown in Figure 6B, the full-length SVIP was associated with membranes and not released from permeabilized cells, whereas the N-terminal deletion mutant was located in both the cytoplasm and nucleus, and was mark-
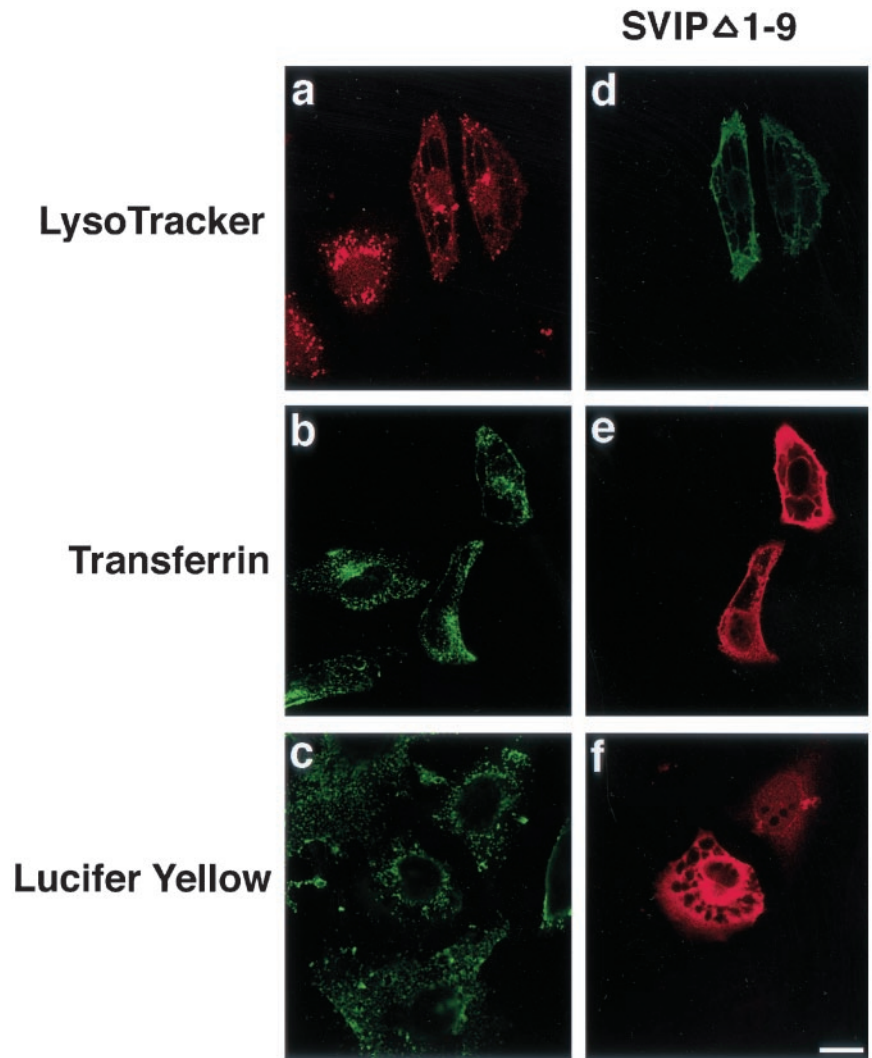
SVIP△1-9

Figure 8. Large vacuoles in SVIP-expressing cells are not derived from endosomal and/or lysosomal compartments. Cells transfected with the plasmid for C-terminally FLAG-tagged SVIPΔ1-9 were incubated with 100 nM LysoTracker for 30 min (a), 25 μg/ml transferrin for 1 h (b), or 5 mg/ml lucifer yellow for 5 min (c). To localize SVIPΔ1-9–expressing cells, cells were immunostained with anti-FLAG (d, e, and f). Antibodies against transferrin and lucifer yellow were used for immunostaining.

edly, but perhaps not completely, released from permeabilized cells, suggesting that the N-terminal region of SVIP functions as a membrane anchor.

Expression of SVIP Induces Formation of Large Vacuoles

We noticed aberrant cellular structures in SVIPΔ1-9–expressing cells (Figure 6B). Immunostaining for an ER membrane protein, NADPH-cytochrome P450 reductase, revealed the formation of large vacuoles (Figure 7a). Expression of the full-length SVIP fused to the C-terminal FLAG also caused cell vacuolation (Figure 10a), albeit to a lesser extent compared with in the case of the mutant. Similar vacuolation was observed when untagged SVIP (Figure 10b) or SVIP fused to the N-terminal GST (Figure 10c) was expressed. These results suggest that vacuolation takes place in SVIP-expressing cells regardless of whether SVIP is membrane associated or not.

Because VCP/p97 is involved in the assembly of Golgi membranes (Rabouille *et al.*, 1995; Kondo *et al.*, 1997), the

Golgi structure may be perturbed by the expression of SVIP. When the Golgi structure was observed by immunostaining of cells with antibodies against β-COP, a Golgi coat protein, and γ-adaptin, a *trans*-Golgi network protein, no significant change was detected (Figure 7, b and c). Similarly, no change was observed in microtubules (Figure 7d).

We examined whether the large vacuoles formed are derived from the endosomal and/or lysosomal compartments. For this purpose, acidic organelles in SVIP-expressing cells were stained with LysoTracker. As shown in Figure 8a, LysoTracker was not detected inside the large vacuoles. In addition, transferrin and lucifer yellow, both of which are frequently used for endocytosis assays, were normally incorporated into cells, and the incorporated dyes were not observed inside the large vacuoles (Figure 8, b and c). These results suggest that the large vacuoles observed in SVIP-expressing cells are not related to endosomal or lysosomal compartments.

Next, we analyzed the vacuoles by electron microscopy. As shown in Figure 9a, ribosomes were frequently observed
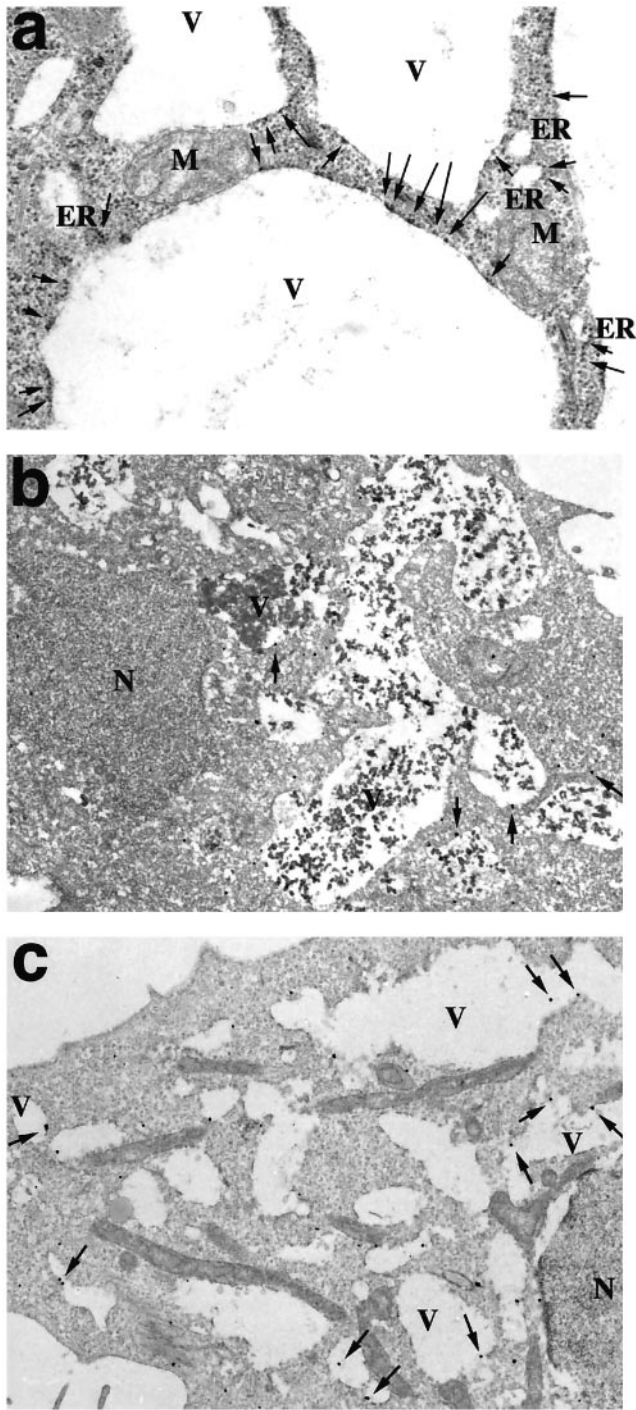
Figure 9. Electron microscopic analysis of vacuoles. (a) Electron microscopic analysis of HeLa cells expressing C-terminally FLAG-tagged SVIPΔ1-9. Arrows indicate ribosomes attached to the vacuole membranes. (b and c) Immunoelectron microscopic analysis of HeLa cells expressing C-terminally FLAG-tagged SVIPΔ1-9 by using the antibody against NADPH-cytochrome P450 reductase (FP2) (b) or BiP (c). Arrows indicate gold particles. The nuclei (N), mitochondria (M), vacuoles (V), and ER are indicated.

on the cytosolic side of vacuole membranes. This may suggest that the large vacuoles are derived from the ER. Consistent with this idea, immunoelectron microscopy showed that an ER membrane protein, NADPH-cytochrome P450 reductase, was located on the vacuole membranes (Figure 9b). If these vacuoles are really derived from the ER, ER lumenal proteins must be present inside them. Figure 9c shows this to be the case. An ER lumenal protein, BiP, was detected inside the vacuoles. The electron-dense materials observed in the vacuoles (Figure 9b) may represent aggregates of lumenal ER proteins.

Formation of Large Vacuoles May Not Be Due to Lack of VCP/p97 Availability in VCP/p97-mediated Pathways

As shown in Figure 10, vacuolation took place when the C-terminally FLAG-tagged full-length SVIP (a) or untagged SVIP (b) was expressed. Expression of the N-terminally GST-tagged SVIP also induced cell vacuolation (c). On the other hand, vacuolation did not occur when the N-terminal region (residues 1–39) of SVIP, which is responsible for the interaction with VCP/p97, or the C-terminal region (residues 40–76) was expressed as a fusion protein with the N-terminal GST (our unpublished data), suggesting that both the N- and C-terminal regions are required to induce cell vacuolation.

Given the involvement of VCP/p97 in many different pathways, the formation of large vacuoles may be due to a shortage of VCP/p97 available for other adaptors as a consequence of the overexpression of SVIP. To examine this possibility, we analyzed the morphology of cells overexpressing other adaptors, p47, and Ufd1p. We reasoned that overexpression of p47 or Ufd1p, like that of SVIP, might induce cell vacuolation by decreasing the amount of VCP/p97 available for adaptor(s) whose disfunction causes cell vacuolation. As shown in Figure 10, overexpression of p47 (d) or Ufd1p (e) did not induce cell vacuolation, suggesting that the formation of vacuoles induced by SVIP overexpression is not simply due to a shortage of VCP/p97.

DISCUSSION

VCP/p97 is involved in diverse cellular functions, and this versatility seems to be conferred by adaptor proteins. To understand the mechanisms underlying VCP/p97-mediated cellular processes, we searched for novel VCP/p97 adaptors by using the yeast two-hybrid system and obtained two classes of positive clones. One class encodes p47, which is known to interact with VCP/p97 (Kondo *et al.*, 1997). The other class encodes a novel protein that we named SVIP. SVIP contains putative myristoylation and palmitoylation sites at the N terminus. Consistent with this fact, endogenous SVIP, albeit lacking transmembrane segments, was associated with membranes. Deletion of the lipid modification sites caused the resultant SVIP to be present in the cytosol.

Binding experiments with mammalian cells revealed that the N-terminal region of SVIP, which contains a putative coiled-coil region, is responsible for the interaction with VCP/p97. On the other hand, the region encompassing the N-terminal and subsequent ATP-binding regions (ND1) of
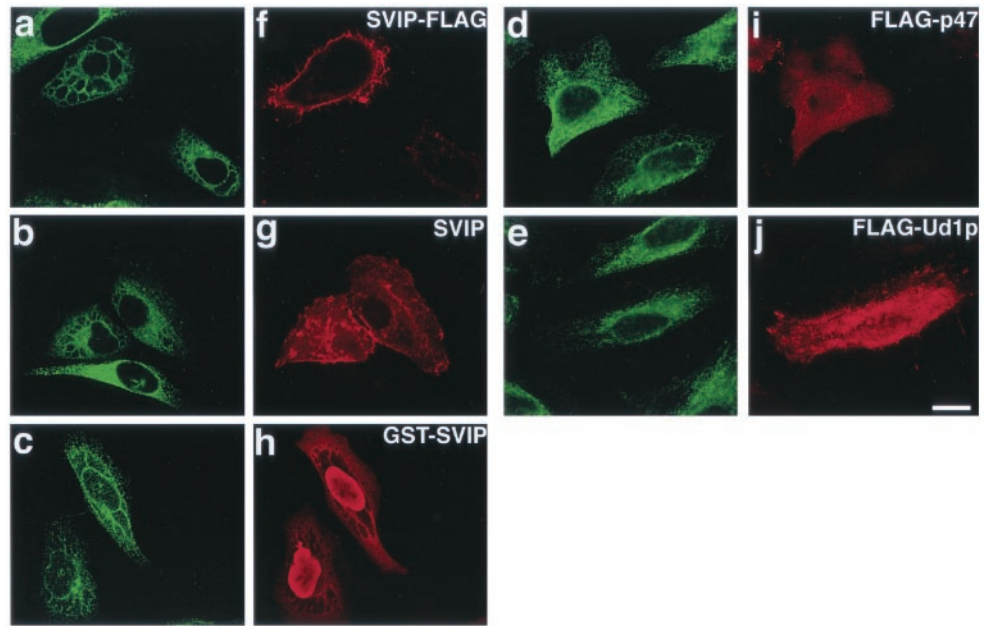
Figure 10. Overexpression of p47 or Ufd1p does not induce cell vacuolation. The C-terminally FLAG-tagged full-length SVIP (a and f), untagged SVIP (b and g), SVIP fused to the N-terminal GST (c and h), N-terminally FLAG-tagged p47 (d and i), or N-terminally FLAG-tagged Ufd1p (e and j) was expressed in HeLa cells. The cells were double stained with the antibodies against BiP (a–e), and FLAG (f, i, and j), SVIP (g), or GST (h).

VCP/p97 is involved in the association with SVIP. It should be noted that p47 and Ufd1p also bind to the ND1 domain. These findings are consistent with the fact that SVIP, p47, and Ufd1p form distinct complexes with VCP/p97. Individual adaptors would occupy the same site on VCP/p97, thereby preventing the binding of other adaptors. This possibility was directly confirmed by the finding that the binding of VCP/p97 to SVIP is inhibited by p47 or Ufd1p in a competitive manner.

Given the fact that the N or D1 domain alone does not bind SVIP, the binding site for SVIP on VCP/p97 may be located between these two domains. An x-ray crystallographic analysis revealed the presence of a large space comprising the area between the β barrel of the N domain and the D1 α helical domain (Zhang et al., 2000a). This space may accommodate the N-terminal α helix of SVIP. Alternatively, the D1 domain coupled with ATP binding and/or hydrolysis may induce a conformational change in the N domain leading to interaction with SVIP. Cryoelectron microscopic observation showed that p47 binds to the periphery of ring-shaped VCP/p97 (Rouiller et al., 2000), suggesting that the surface of the N domain, but not the interface between the N and D1 domains, is involved in the association with p47.

The interaction between VCP/p97 and adaptors is reminiscent of that between NSF and α-soluble NSF attachment protein (SNAP). NSF possesses two ATP-binding regions (D1 and D2) and an N-terminal (N) domain (Tagaya et al., 1993), and belongs to the AAA ATPase family, as VCP/p97 does. The isolated N domain does not bind to α-SNAP, whereas ND1 or ND2 does (Nagiec et al., 1995). It has been speculated that the C-terminal α-helix of α-SNAP is positioned toward the D1 domain through a groove in the N domain of NSF (Yu et al., 1999). Thus, AAA family proteins in general may bind adaptor molecules at the interface between the N-terminal and ATP-binding regions. The fact that nearly half of the residues implicated in the interaction between the N and D1 domains are conserved between NSF

and VCP/p97 (May et al., 1999; Yu et al., 1999) may support this idea.

Overexpression of the full-length SVIP or SVIPΔ1-9 caused the formation of aberrant large vacuoles. The vacuoles seemed to be enlarged ERs, but not to be derived from endosomal and/or lysosomal acidic compartments. In this respect, SVIP-induced cell vacuolation is obviously different from that induced by *Helicobacter pylori* (de Bernard et al., 1998). Vacuoles induced by *H. pylori* infection are enlarged endosomal and/or lysosomal compartments (de Bernard et al., 1998). How does vacuolation take place when SVIP is overexpressed? At present, there are no available data that allow us to speculate on the mechanism underlying vacuolation. However, analysis of the mechanism underlying vacuolation may provide an insight into the mechanism underlying neuronal cell death. Vacuoles induced by the overexpression of SVIP are reminiscent of those induced by abnormal protein aggregates in neuronal cells. Recently, Hirabayashi et al. (2001) reported that VCP/p97, by interacting with polyglutamine proteins, is involved in cell death relevant to neurodegeneration. Certain neurodegenerative disorders such as Huntington disease involve accompanying vacuolation of neuronal cells. Overexpression of a VCP/p97 mutant, which is supposed to lack ATPase activity, causes the formation of vacuoles that may originate from the ER (Hirabayashi et al., 2001).

ACKNOWLEDGMENTS

REFERENCES

Acharya, U., Jacobs, R., Peters, J.M., Watson, N., Farquhar, M.G., and Malhotra, V. (1995). The formation of Golgi stacks from vesiculated Golgi membranes requires two distinct fusion events. Cell *82*, 895–904.

Bays, N.W., Wilhovsky, S.K., Goradia, A., Hodgkiss-Harlow, K., and Hampton, R.Y. (2001). HRD4/NPL4 is required for the proteasomal processing of ubiquitinated ER proteins. Mol. Biol. Cell *12*, 4114–4128.

Boehmelt, G., *et al*. (2000). Cloning and characterization of the murine glucosamine-6-phosphate acetyltransferase EMeg32. Differential expression and intracellular membrane association. J. Biol. Chem. *275*, 12821–12832.

Braun, S., Matuschewski, K., Rape, M., Thoms, S., and Jentsch, S. (2002). Role of the ubiquitin-selective CDC48UFD1/NPL4 chaperone (segregase) in ERAD of OLE1 and other substrates. EMBO J. *21*, 615–621.

Confalonieri, F., and Duguet, M. (1995). A 200-amino acid ATPase module in search of a basic function. Bioessays *17*, 639–650.

Cruciat, C.M., Hell, K., Folsch, H., Neupert, W., and Stuart, R.A. (1999). Bcs1p, an AAA-family member, is a chaperone for the assembly of the cytochrome bc_1 complex. EMBO J. *18*, 5226–5233.

Dai, R.M., Chen, E., Longo, D.L., Gorbea, C.M., and Li, C.-C.H. (1998). Involvement of valosin-containing protein, an ATPase co-purified with IκBα and 26 S proteasome, in ubiquitin-proteasome-mediated degradation of IκBα. J. Biol. Chem. *273*, 3562–3573.

Dai, R.M., and Li. C.-C.H. (2001). Valosin-containing protein is a multi-ubiquitin chain-targeting factor required in ubiquitin-proteasome degradation. Nat. Cell Biol. *3*, 740–744.

de Bernard, M., Moschioni, M., Papini, E., Telford, J., Rappuoli, R., and Montecucco, C. (1998). Cell vacuolization induced by *Helicobacter pylori* VacA toxin: cell line sensitivity and quantitative estimation. Toxicol. Lett. *99*, 109–115.

DeHoratius, C., and Silver, P.A. (1996). Nuclear transport defects and nuclear envelope alterations are associated with mutation of the *Saccharomyces cerevisiae* NPL4 gene. Mol. Biol. Cell *7*, 1835–1855.

Egerton, M., Ashe, O.R., Chen, D., Druker, B.J., Burgess, W.H., and Samelson, L.E. (1992). VCP, the mammalian homolog of cdc48, is tyrosine phosphorylated in response to T cell antigen receptor activation. EMBO J. *11*, 3533–3540.

Ghislain, M., Dohmen, R.J., Levy, F., and Varshavsky, A. (1996). Cdc48p interacts with Ufd3p, a WD repeat protein required for ubiquitin-mediated proteolysis in *Saccharomyces cerevisiae*. EMBO J. *15*, 4884–4899.

Golbik, R., Lupas, A.N., Koretke, K.K., Baumeister, W., and Peters, J. (1999). The Janus face of the archaeal Cdc48/p97 homologue VAT: protein folding versus unfolding. J. Biol. Chem. *380*, 1049–1062.

Hanson, P.I., Roth, R., Morisaki, H., Jahn, R., and Heuser, J.E. (1997). Structure and conformational changes in NSF and its membrane receptor complexes visualized by quick-freeze/deep-etch electron microscopy. Cell *90*, 523–535.

Hatsuzawa, K., Hirose, H., Tani, K., Yamamoto, A., Scheller, R.H., and Tagaya, M. (2000). Syntaxin 18, a SNAP receptor that functions in the endoplasmic reticulum, intermediate compartment, and *cis*-Golgi vesicle trafficking. J. Biol. Chem. *275*, 13713–13720.

Hetzer, M., Meyer, H.H., Walther, T.C., Bilbao-Cortes, D., Warren, G., and Mattaj, I.W. (2001). Distinct AAA-ATPase p97 complexes function in discrete steps of nuclear assembly. Nat. Cell Biol. *3*, 1086–1091.

Hirabayashi, M., *et al*. (2001). VCP/p97 in abnormal protein aggregates, cytoplasmic vacuoles, and cell death, phenotypes relevant to neurodegeneration. Cell Death Diff. *8*, 977–984.

Hitchcock, A.L., Krebber, H., Frietze, S., Lin, A., Latterich, M., and Silver, P.A. (2001). The conserved Npl4 protein complex mediates proteasome-dependent membrane-bound transcription factor activation. Mol. Biol. Cell *12*, 3226–3241.

Jarosch, E., Taxis, C., Volkwein, C., Bordallo, J., Finley, D., Wolf, D.H., and Sommer, T. (2002). Protein dislocation from the ER requires polyubiquitination and the AAA-ATPase Cdc48. Nat. Cell Biol. *4*, 134–139.

Johnson, E.S., Ma, P.C., Ota, I.M., and Varshavsky, A. (1995). A proteolytic pathway that recognizes ubiquitin as a degradation signal. J. Biol. Chem. *270*, 17442–17456.

Koegl, M., Hoppe, T., Schlenker, S., Ulrich, H.D., Mayer, T.U., and Jentsch, S. (1999). A novel ubiquitination factor, E4, is involved in multiubiquitin chain assembly. Cell *96*, 635–644.

Koller, K.J., and Brownstein, M.J. (1987). Use of a cDNA clone to identify a supposed precursor protein containing valosin. Nature *325*, 542–545.

Kondo, H., Rabouille, C., Newman, R., Levine, T.P., Pappin, D., Freemont, P., and Warren, G. (1997). p47 is a cofactor for p97-mediated membrane fusion. Nature *388*, 75–78.

Latterich, M., Frohlich, K.-U., and Schekman, R. (1995). Membrane fusion and the cell cylce: Cdc48p participates in the fusion of ER membranes. Cell *82*, 885–893.

Lavoie, C., Chevet, E., Roy, L., Tonks, N.K., Fazel, A., Posner, B.I., Paiement, J., and Bergeron, J.J. (2000). Tyrosine phosphorylation of p97 regulates transitional endoplasmic reticulum assembly in vitro. Proc. Natl. Acad. Sci. USA *97*, 13637–13642.

Leon, A., and McKearin, D. (1999). Identification of TER94, an AAA ATPase protein, as a Bam-dependent component of the *Drosophila* fusome. Mol. Biol. Cell *10*, 3825–3834.

Leonhard, K., Stiegler, A., Neupert, W., and Langer, T. (1999). Chaperone-like activity of the AAA domain of the yeast Yme1 AAA protease. Nature *398*, 348–351.

Lupas, A., Van Dyke, M., and Stock, J. (1991). Predicting coiled coils from protein sequences. Science *252*, 1162–1164.

Masaki, R., Yamamoto, A., and Tashiro, Y. (1987). Cytochrome P-450 and NADPH-cytochrome P-450 reductase are degraded in the autolysosomes in rat liver. J. Cell Biol. *104*, 1207–1215.

May, A.P., Misura, K.M., Whiteheart, S.W., and Weis, W.I. (1999). Crystal structure of the amino-terminal domain of *N*-ethylmaleimide-sensitive fusion protein. Nat. Cell Biol. *1*, 175–182.

Meyer, H.H., Shorter, J.G., Seemann, J., Pappin, D., and Warren, G. (2000). A complex of mammalian Ufd1 and Npl4 links the AAA-ATPase, p97, to ubiquitin and nuclear transport pathways. EMBO J. *19*, 2181–2192.

Morgan, A., and Burgoyne, R.D. (1995). Is NSF a fusion protein? Trends Cell Biol. *5*, 335–339.

Nagiec, E.E., Bernstein, A., and Whiteheart, S.W. (1995). Each domain of the *N*-ethylmaleimide-sensitive fusion protein contributes to its transport activity. J. Biol. Chem. *270*, 29182–29188.

Nakamura, N., Yamamoto, A., Wada, Y., and Futai, M. (2000). Syntaxin 7 mediates endocytic trafficking to late endosomes. J. Biol. Chem. *275*, 6523–6529.

Neuwald, A.F., Aravind, L., Spouge, J.L., and Koonin, E.V. (1999). AAA+: a class of chaperone-like ATPases associated with the assembly, operation, and disassembly of protein complexes. Genome Res. *9*, 27–43.

Ogura, T., and Wilkinson, A.J. (2001). AAA$^+$ superfamily ATPases: common structure-diverse function. Genes Cells 6, 575–597.

Patel, S., and Latterich, M. (1998). The AAA team: related ATPases with diverse functions. Trends Cell Biol. 8, 65–71.

Pleasure, I.T., Black, M.M., and Keen, J.H. (1993). Valosin-containing protein, VCP, is a ubiquitous clathrin-binding protein. Nature 365, 459–462.

Rabinovich, E., Kerem, A., Frohlich, K.U., Diamant, N., and Bar-Nun, S. (2002). AAA-ATPase p97/Cdc48p, a cytosolic chaperone required for endoplasmic reticulum-associated protein degradation. Mol. Cell. Biol. 22, 626–634.

Rabouille, C., Kondo, H., Newman, R., Hui, N., Freemont, P., and Warren, G. (1998). Syntaxin 5 is a common component of the NSF- and p97-mediated reassembly pathways of Golgi cisternae from mitotic Golgi fragments in vitro. Cell 92, 603–610.

Rabouille, C., Levine, T.P., Peters, J.M., and Warren, G. (1995). An NSF-like ATPase, p97, and NSF mediate cisternal regrowth from mitotic Golgi fragments. Cell 82, 905–914.

Rape, M., Hoppe, T., Gorr, I., Kalocay, M., Richly, H., and Jentsch, S. (2001). Mobilization of processed, membrane-tethered SPT23 transcription factor by CDC48$^{UFD1/NPL4}$, a ubiquitin-sensitive chaperone. Cell 107, 667–677.

Rouiller, I., Butel, V.M., Latterich, M., Milligan, R.A., and Wilson-Kubalek, E.M. (2000). A major conformational change in p97 AAA ATPase upon ATP binding. Mol. Cell 6, 1485–1490.

Roy, L., Bergeron, J.J., Lavoie, C., Hendriks, R., Gushue, J., Fazel, A., Pelletier, A., Morre, D.J., Subramaniam, V.N., Hong, W., and Paiement, J. (2000). Role of p97 and syntaxin 5 in the assembly of transitional endoplasmic reticulum. Mol. Biol. Cell 11, 2529–2542.

Ruden, D.M., Sollars, V., Wang, X., Mori, D., Alterman, M., and Lu, X. (2000). Membrane fusion proteins are required for oskar mRNA localization in the Drosophila egg chamber. Dev. Biol. 218, 314–325.

Schulte, R.J., Campbell, M.A., Fischer, W.H., and Sefton, B.M. (1994). Tyrosine phosphorylation of VCP, the mammalian homologue of the Saccharomyces cerevisiae CDC48 protein, is unusually sensitive to stimulation by sodium vanadate and hydrogen peroxide. J. Immunol. 153, 5465–5472.

Shirogane, T., Fukada, T., Muller, J.M., Shima, D.T., Hibi, M., and Hirano, T. (1999). Synergistic roles for Pim-1, and c-Myc in STAT3-mediated cell cycle progression, and antiapoptosis. Immunity 11, 709–719.

Sugita, S., and Südhof, T.C. (2000). Specificity of Ca^{2+}-dependent protein interactions mediated by C$_2$A domains of synaptotagmin. Biochemistry 39, 2940–2949.

Tagaya, M., Furuno, A., and Mizushima, S. (1996). SNAP prevents Mg^{2+}-ATP-induced release of N-ethylmaleimide-sensitive factor from the Golgi apparatus in digitonin-permeabilized PC12 cells. J. Biol. Chem. 271, 466–470.

Tagaya, M., Wilson, D.W., Brunner, M., Arango, N., and Rothman, J.E. (1993). Domain structure of an N-ethylmaleimide-sensitive fusion protein involved in vesicular transport. J. Biol. Chem. 268, 2662–2666.

Tanaka, M., Gupta, R., and Mayer, B.J. (1995). Differential inhibition of signaling pathways by dominant-negative SH2/SH3 adapter proteins. Mol. Cell. Biol. 15, 6829–6837.

Vale, R.D. (2000). AAA proteins: lords of the ring. J. Cell Biol. 150, F13–F20.

Wu, X.-Q., Lefrancois, S., Morales, C., and Hecht, N.B. (1999). Protein-protein interaction between the testis brain RNA-binding protein and the transitional endoplasmic reticulum ATPase, a cytoskeletal γ actin and Trax in male germ cells and the brain. Biochemistry 38, 11261–11270.

Yamada, T., Okuhara, K., Iwamatsu, A., Seo, H., Ohta, K., Shibata, T., and Murofushi, H. (2000). p97 ATPase, an ATPase involved in membrane fusion, interacts with DNA unwinding factor (DUF) that functions in DNA replication. FEBS Lett. 466, 287–291.

Yamaguchi, T., Yamamoto, A., Furuno, A., Hatsuzawa, K., Tani, K., Himeno, M., and Tagaya, M. (1997). Possible involvement of heterotrimeric G proteins in the organization of the Golgi apparatus. J. Biol. Chem. 272, 25260–25266.

Ye, Y., Meyer, H.H., and Rapoport, T.A. (2001). The AAA ATPase Cdc48/p97 and its partners transport proteins from the ER into the cytosol. Nature 414, 652–656.

Yen, C.H., Yang, Y.C., Ruscetti, S.K., Kirken, R.A., Dai, R.M., and Li, C.-C.H. (2000). Involvement of the ubiquitin-proteasome pathway in the degradation of nontyrosine kinase-type cytokine receptors of IL-9, IL-2, and erythropoietin. J. Immunol. 165, 6372–6380.

Yu, R.C., Jahn, R., and Brunger, A.T. (1999). NSF N-terminal domain crystal structure: models of NSF fusion. Mol. Cell 4, 97–107.

Zhang, L., Ashendel, C.L., Becker, G.W., and Morre, J. (1994). Isolation and characterization of the principal ATPase associated with transitional endoplasmic reticulum. J. Cell Biol. 127, 1871–1883.

Zhang, X., et al. (2000a). Structure of the AAA ATPase p97. Mol. Cell 6, 1473–1484.

Zhang, H., Wang, Q., Kajino, K., and Greene, M.I. (2000b). VCP, a weak ATPase involved in multiple cellular events, interacts physically with BRCA1 in the nucleus of living cells. DNA Cell Biol. 19, 253–263.